ORIGINAL ARTICLE

CrossMark

The influence of porcine epidemic diarrhea virus on pig small intestine mucosal epithelial cell function

Xing-Ye Wang[1] · Tai-Qiang Zhao[2] · De-Peng Xu[1] · Xue Zhang[1] · Cheng-Jie Ji[2] · De-Li Zhang[1]

Abstract

Porcine epidemic diarrhea (PED) is a highly contagious, acute enteric tract infectious disease of pigs (*Sus domesticus*) caused by porcine epidemic diarrhea virus (PEDV). PED is characterized by watery diarrhea, dehydration, weight loss, vomiting and death. PEDV damages pig intestinal epithelial tissue, causing intestinal hyperemia and atrophy of intestinal villi, with formation of intestinal epithelial cell cytoplasmic vacuoles. Since pig small intestinal epithelial cells (IECs) are target cells of PEDV infection, IEC cells were utilized as a model for studying changes in cellular activities post-PEDV infection. Monitoring of Na^+-K^+-ATPase and Ca^{2+}-Mg^{2+}-ATPase activities demonstrated that PEDV infection decreased these activities. In addition, IECs proliferation was shown to decrease after PEDV infection using an MTT assay. Moreover, IECs apoptosis detected by flow cytometry with propidium iodide (PI) staining was clearly shown to increase relative to the control group. Meanwhile, animal experiments indicated that PEDV virulence for IEC cells was greater than viral virulence for Vero cells, although this may be due to viral attenuation after numerous passages in the latter cell line. Collectively, these studies revealed viral pathogenic mechanisms in PEDV-infected IECs and offer a theoretical basis for PEDV prevention and control.

Introduction

Porcine epidemic diarrhea virus (PEDV) is the etiologic agent that causes porcine epidemic diarrhea. This virus was first discovered in England in 1971 and was later identified as a member of *Coronaviridae* [1, 2]. PEDV causes severe diarrhea and dehydration, resulting in 100% morbidity and roughly 80% to 100% mortality in piglets [3–5]. Although great progress has been made in molecular epidemiology, diagnosis, treatment and prevention of PED [6, 7], frequencies of outbreaks of this virus continue to rise, causing

---

Xing-Ye Wang and Tai-Qiang Zhao contributed equally to this work.

✉ Cheng-Jie Ji
  iburningji@gmail.com

✉ De-Li Zhang
  zhangdeli@tsinghua.org.cn

[1] College of Veterinary Medicine, Northwest A&F University, 22 Xinong Road, Yangling District, Shaanxi 712100, China

[2] Department of Laboratory Medicine, Sichuan Academy of Medical Science and Sichuan Provincial People's Hospital, Chengdu 610072, Sichuan, China

problems for the swine industry and for international trade. Indeed, outbreaks in the US and other countries have been caused by virus variants that are very similar to the Chinese AH2012 strain [8, 9], suggesting that global transmission is already underway.

Very few cell lines or primary cells have been found to support PEDV replication. Subsequently, most research on this virus has been conducted using Vero and Marc-145 cell lines, which are derived from cells originally isolated from monkey kidney [10]. These cell lines greatly differ from the natural host of PEDV replication, porcine intestinal epithelial cells (IECs). A model to investigate the interaction between porcine small intestinal epithelial cells and PEDV is badly needed to increase understanding of viral molecular mechanisms underlying virulence, pathogenesis and disease treatment. Recent study showed that IPEC-J2 from DSMZ (No: ACC701) and IECs from China can be infected with PEDV [11, 12], but still little is known about the interaction between porcine IECs and PEDV.

Small intestinal mucosal epithelial cell membrane integrity is an important function that maintains the structure and function of the small bowel and depends on membrane protein functions of constituent cells [13–15]. Na^+-K^+-ATPase and Ca^{2+}-Mg^{2+}-ATPase are special proteins located within cell membranes that help to maintain ion balances inside

and outside cells using ion transport [16]. Studies have revealed that abnormal functioning of ATPases precedes the occurrence of certain diseases, with abnormal degrees of enzyme dysfunction positively correlated with disease severity [17, 18]. PED clinical features, including watery diarrhea, dehydration and weight loss in pigs mainly result from interference with normal small intestinal function stemming from viral infection. Therefore, Na^+-K^+-ATPase and Ca^{2+}-Mg^{2+}-ATPase activities are likely to be relevant to PEDV pathogenesis and can be used as tools to study pathogenic mechanisms.

Numerous intestinal pathogenic factors, such as bacteria or viruses, are known to cause severe diarrhea in humans and animals [19, 20]. Because the use of animals as infection models to study PEDV pathogenic mechanisms can be cumbersome, an appropriate cell line for *in vitro* studies is urgently needed. In this study, IECs were isolated from piglets at 12 hours after birth and the cells were passaged *in vitro* with no loss of epithelioid characteristics [12]. IECs were next used to study changes in pig small intestinal mucosa epithelial cell activities after PEDV infection, revealing essential PEDV pathogenic infection mechanisms and providing valuable information for the prevention, treatment and control of porcine epidemic diarrhea.

Materials and methods

Swine

Nine 10-day-old healthy Landrace piglets that tested negative for RV (rotavirus), TGEV (transmissible gastroenteritis coronavirus) and PEDV were purchased from Yiyang Piglet Farm (Shaanxi, China). All animal experiments were carried out in compliance with current Chinese ethical guidelines.

Cell lines, PEDV strain

Vero cells (ATCC CCL-81) are cells originally derived from African green monkey kidney cells. Immortalized pig small intestinal mucosal epithelial cells were contributed by Prof. Yan-Ming Zhang, College of Veterinary Medicine, Northwest A&F University [12]. Both cell types were cultured with Dulbecco's Modified Eagle Medium (DMEM) supplemented with 10% fetal bovine serum (FBS), 100 µg/ml penicillin and 100 µg/ml streptomycin. The PEDV CV777 strain was provided by the Chinese National Center for Animal Health and Animal Epidemiology.

Reagents

DMEM containing high glucose and FBS were purchased from Gibco (Gaithersburg, MD, USA). PEDV N protein-specific monoclonal antibody was purchased from Medgene Labs (Brookings, SD, USA). Horseradish peroxidase (HRP)-conjugated goat anti-mouse IgG secondary antibody was purchased from Tianjin Sungene Biotech Co. (Tianjin, China). The Ultramicro ATPases checkerboard was purchased from Nanjing Jiancheng Bioengineering Institute (Nanjing, Jiangsu Province, China); Easy II Protein Quantitative Kit (BCA) was purchased from TransGen Biotech (Beijing, China); 3-(4,5-dimethylthiazol-2-yl)-2,5-diphenyltetrazolium bromide (MTT) was purchased from TransGen Biotech (China). Working concentration binding buffer and annexin V-PE/PI were purchased from Abcam (Cambridge, MA, USA).

Immunofluorescence assay (IFA)

PEDV-infected IECs on cover glasses were permeabilized with 1% Triton X-100 for 10 minutes and blocked with 2% bovine serum albumin (BSA) for 10 minutes. Infected cells were then incubated with PEDV N-monoclonal antibody for 30 minutes followed by incubation with fluorescein-conjugated goat anti-mouse IgG (Rockland Immunochemicals Inc., Limerick, PA, USA). Each cover glass was mounted on a slide and stained cells were observed under confocal microscopy after addition of SlowFade Gold Antifade Reagent containing 4',6-diamidino-2-phenylindole (DAPI) (Life Technologies Corp., Carlsbad, CA, USA).

Western blot analysis

Cell samples were lysed using lysis buffer and boiled in SDS sample buffer for 15 minutes. Protein quantity was detected using the Easy II Protein Quantitative Kit (TransGen Biotech, Beijing, China) and equal amounts of total protein were loaded onto SDS-polyacrylamide gels and separated electrophoretically then transferred onto polyvinylidene fluoride membranes (Millipore, Burlington, MA, USA). After incubation with primary and secondary antibodies, protein bands were visualized using Luminata Classico Western HRP Substrate (Millipore, USA) according to the manufacturer's instructions.

50% cell culture infectious dose (TCID 50) assay

Vero cells were seeded into clear 96-well plates at 10^4 cells per well in 100 µl of DMEM containing 10% FBS; cells were seeded into all wells except column 10, which was left

empty to separate infected cell wells from uninfected cell wells. After 12 hours, serial dilutions of virus (1:10 from 10^{-1} to 10^{-9}) each containing 5% trypsin were prepared. After discarding cell supernatants, 100 µl of each virus dilution was added to columns 1 to 9 in order from 10^{-1} to 10^{-9}, respectively. Pipette tips were changed between columns. Columns 11 and 12 contained medium only and served as controls. The plates were then incubated at 37 °C with 5% CO_2 for 6 days. On the 6th day, supernatants were discarded and cells were fixed for 15 minutes at room temperature. Next, supernatants were removed and cells were examined for cytopathic effect (CPE) via IFA methods and the numbers of positive wells for CPE were scored. A Reed and Muench calculation [21] was then performed to determine the TCID50, which was then presented as TCID50 per ml.

Cell viability assessment

IEC viability values after PEDV infection were determined by MTT assay, which was monitored by evaluating mitochondrial damage that occurs upon cell death, as previously described [22]. Briefly, 1×10^4 cells per well were seeded into 96-well plates and infected with PEDV at various multiplicity of infection (MOI) values (0.1, 0.5, 1, 2, 4 MOI) for 24, 48, 72, 96 or 120 hours. Meanwhile, negative controls and blank controls were set up. 5 mg/ml of MTT was added to per well and incubated at 37 °C for 4 hours. Next, dimethyl sulfoxide (DMSO) was added and the absorbance was measured using a microplate spectrophotometer (Infinite 200 PRO NanoQuant, Tecan, Switzerland) at 570 nm. Results show the means $\pm$ SEM of three experiments performed in quintuplicate.

Na$^+$-K$^+$-ATPase and Ca^{2+}-Mg^{2+}-ATPase activity analyses

Cells were collected after 0, 24, 48, 72, 96 or 120 hours post-infection (hpi) using 0.1 MOI of CV777. The total cell protein concentration was detected after three freeze-thaw cycles. Na$^+$-K$^+$-ATPase and Ca^{2+}-Mg^{2+}-ATPase quantities relative to total cell protein were then measured using a commercial kit according to the manufacturer's instructions (Nanjing Jiancheng Bioengineering Institute, Jiangsu, China). One ATPase activity unit is defined as 1 µmol of phosphate generated by the hydrolysis of ATP catalyzed by ATPase per 1 mg of total cell protein.

Cell apoptosis assay

IECs were harvested at 18 hpi via detachment using trypsin and approximately 5×10^5 cells for each treatment group were then resuspended in working concentration binding buffer (Abcam, USA) and incubated with annexin V-PE/

PI (Abcam, USA) for 15 minutes at 4 °C. The extent of apoptosis was quantified by flow cytometry (FACS LSRII; Becton Dickinson, San Jose, CA). Dead cells and debris were excluded by selective gating based on electronic cell volume determination. About 20000 events were collected for each sample.

Virulence experiment measuring CV777 proliferation in IEC and Vero cells

Nine 7-day-old piglets were used to evaluate the virulence of the PEDV CV777 strain amplified in IEC and Vero cells. All piglets were negative for RV, TGEV and PEDV as determined using a reverse transcription-polymerase chain reaction (RT-PCR) method. In addition, piglets were shown to be negative for antibody specific for PEDV, as demonstrated using a TRM-556 PEDV ELISA Kit (Biovet, Saint-Hyacinthe, QC, Canada). Piglets were randomly divided into three groups designated group 1, group 2 and group 3. Group 1 and group 2 were orally administered 2 ml CV777 harvested at viral passage 10 in IEC cells or Vero cells, respectively, and were infected using the same virus dose of 10^6 per ml; group 3 pigs were given 2 ml of cell culture medium without virus. Clinical signs were observed daily and necropsy was performed at 4 days post-inoculation. Representative intestinal tissues were fixed in formalin and embedded in paraffin wax using standard methods. The histological paraffin sections were then stained with hematoxylin and eosin (HE) to detect viral effects on piglet small intestinal mucosal layer thickness, villus length and villus/crypt (V/C) ratio, all of which were measured using Motic Images Advanced 3.0 software.

Statistical analyses

Calculation of means and standard deviations (SD) and other statistical analyses were performed using SPSS 18.0. Differences between experimental and control groups were assessed using an independent samples test, with p-values < 0.05 considered statistically significant and p-values < 0.01 considered highly significant.

Results

PEDV infection of IECs in vitro was followed by extensive viral replication

IFA using N protein-specific monoclonal antibody detected PEDV replication in cytosols of cells after infection with 0.1 MOI CV777 (Fig 1A). From the figure, CPE was not obvious but was characterized by cell clumping, cell swelling and rounding up, with cells exhibiting partial detachment

Fig. 1 PEDV replication in IEC cells was detected by IFA (A) and Western Blotting (B). A, IEC cells were infected with CV777 at 1 MOI for 24 hours, PEDV-induced CPE were recorded and cells were examined by IFA using PEDV-specific monoclonal antibody (× 100 magnification). B, PEDV N protein in cells detected by Western blotting, Vero, IEC and Marc-145 cells were inoculated with CV777 at an MOI of 1 for 72 hours
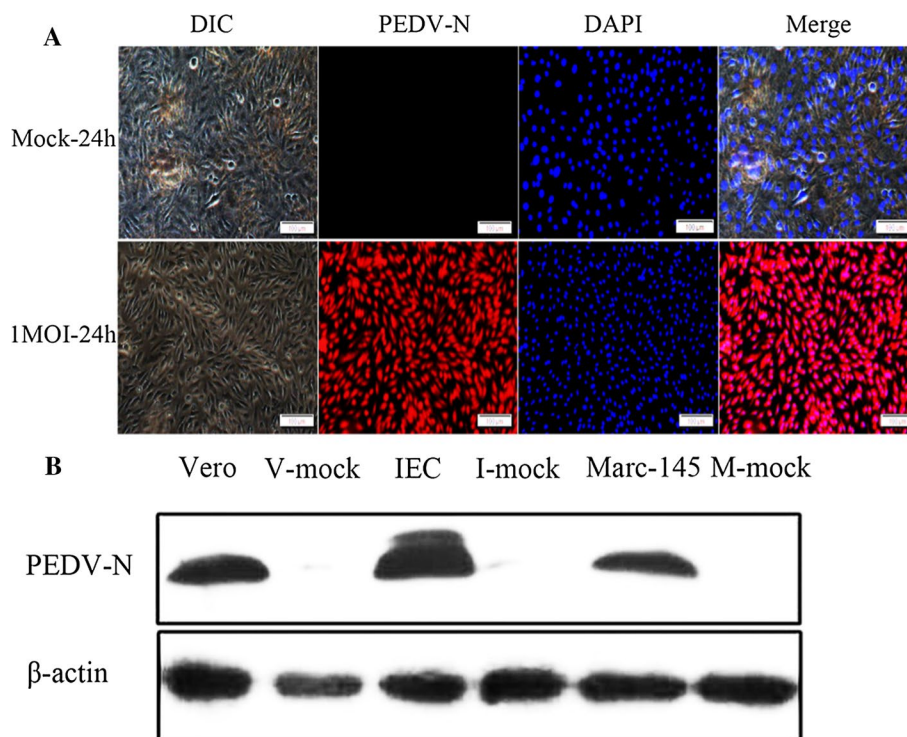
from the substrate. Western blot was performed to detect N protein expression in Vero, IEC and Marc-145 cells after 72 hours post-infection using 0.1 MOI CV777 (Fig 1B). The PEDV strain was shown to propagate in IECs, which were more susceptible to PEDV infection than in Vero and Marc-145 cells.

The PEDV multi-step growth curve exhibited slightly higher virus propagation levels in IECs than in Vero cells

Growth properties of PEDV in IEC cells were determined and differences in virus titer levels between inoculated IECs and Vero cells were assessed after treating cells using 1 MOI of CV777. Virus content was detected by TCID50 at 0, 24, 48, 72, 96 and 120 hpi and the result demonstrated that PEDV exhibited a significantly higher propagation level in IEC cells than in Vero cells after 24 hpi (Table 1).

Changes in Na^+-K^+-ATPase and Ca^{2+}-Mg^{2+}-ATPase activities

Previous studies had shown that virus replication in small intestinal epithelial cells affected the activities of Na^+-K^+-ATPase and Ca^{2+}-Mg^{2+}-ATPase, with inhibition of activities predominantly observed [23]. In this study, the activity of Na^+-K^+-ATPase and Ca^{2+}-Mg^{2+}-ATPase were investigated in response to infection with 0.1 MOI CV777 (Tables 2 and 3). At 0, 24, 48, 72, 96 or 120 hours

Table 1 Virus yield titration of CV777 on IEC cells and Vero cells at various time points. TCID 50 /ml counts for virus titers at a 1:10 dilution for each experiment (repeated five times). n = 5; *P < 0.05; **P < 0.01

Time (hpi)	IEC	Vero
24	4.28×10^4**	3.55×10^4
48	6.31×10^5**	8.91×10^4
72	6.88×10^5**	3.55×10^5
96	7.61×10^6**	7.61×10^5
120	2.82×10^7**	2.82×10^5
144	6.31×10^5**	3.55×10^2

post-infection, the activity of ATPases was measured using optical density (OD) readings. Both ATPase activities were significantly reduced in the infection group compared with the control group. Furthermore, a significant change was detected in Na(+), K(+) and Ca(2+) content that correlated with observed down-regulation of Na^+-K^+-ATPase and Ca^{2+}-Mg^{2+}-ATPase activities. These results demonstrate that infection may cause a water-electrolyte imbalance that may then trigger the watery diarrhea and dehydration typically observed in PED.

PEDV infection inhibition of growth of IEC cells

In order to assess the influence of PEDV on growth of IECs, we investigated the viability of IEC cells at 0, 24, 48, 72, 96 and 120 hpi. We observed a significant inhibition of cellular

Table 2 Na$^+$-K$^+$-ATPase of IECs activity at various time points post-PEDV infection (U/mg protein). n = 6; *P < 0.05; **P < 0.01

Group	Time (hpi)					
	0	24	48	72	96	120
The negative group	6.21 ± 0.03	6.15 ± 0.01	6.10 ± 0.03	5.93 ± 0.05	5.65 ± 0.02	5.53 ± 0.03
The positive group	6.28 ± 0.05	5.77 ± 0.02*	5.02 ± 0.01**	4.09 ± 0.03**	3.35 ± 0.04**	2.97 ± 0.01**

Table 3 Activity of Ca^{2+}-Mg^{2+}-ATPase of IECs infected with PEDV (U/mg protein). n = 6; *P < 0.05; **P < 0.01

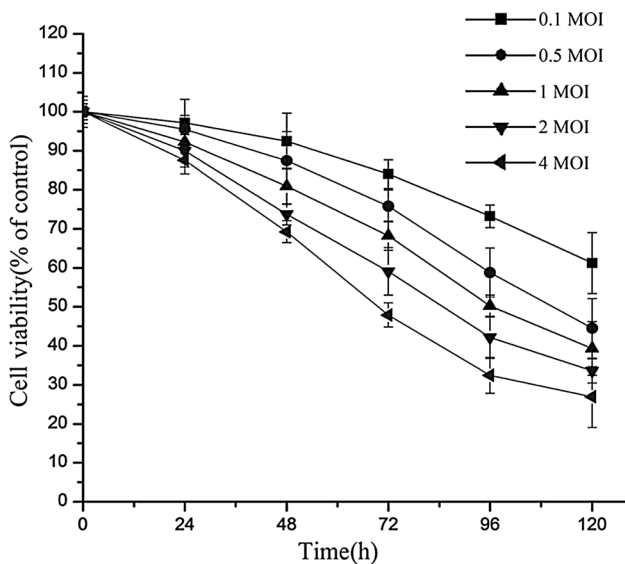| Group	Time (hpi)					
	0	24	48	72	96	120
The negative group	8.40 ± 0.01	8.19 ± 0.03	8.05 ± 0.03	7.71 ± 0.02	7.44 ± 0.01	7.15 ± 0.03
The positive group	8.47 ± 0.03	7.96 ± 0.04*	7.33 ± 0.05**	6.62 ± 0.01**	6.08 ± 0.03**	5.24 ± 0.02**

Fig. 2 The effect of PEDV on cell viability. IEC cells were infected with CV777 at various doses for 0, 24, 48, 72, 96 or 120 hours. Cell viability was measured by MTT assay. The results are means ± SEM and representative of five independent experiments. *P < 0.05, **P < 0.01 versus the control group (not infected)

Fig. 3 Apoptosis rates of PEDV-infected IEC cells. Cells were treated with 0.1 MOI PEDV and stained with annexin V-FITC and PI at indicated time points. Date was analyzed with flow cytometry. Annexin V-positive cells were defined as apoptotic

viability of IECs infected with PEDV at 1.0 MOI, with an increasing trend observed with increase in virus titer and infection time (Fig 2). The result demonstrated that PEDV infection inhibits growth of IECs in a time- and dose-dependent manner.

PEDV infection correlated with increased apoptosis in IECs

To investigate whether apoptosis occurred during PEDV-induced IEC cell death, we observed morphological and molecular changes of IEC cells infected with 0.1 MOI of PEDV at indicated time points. Annexin V and PI staining
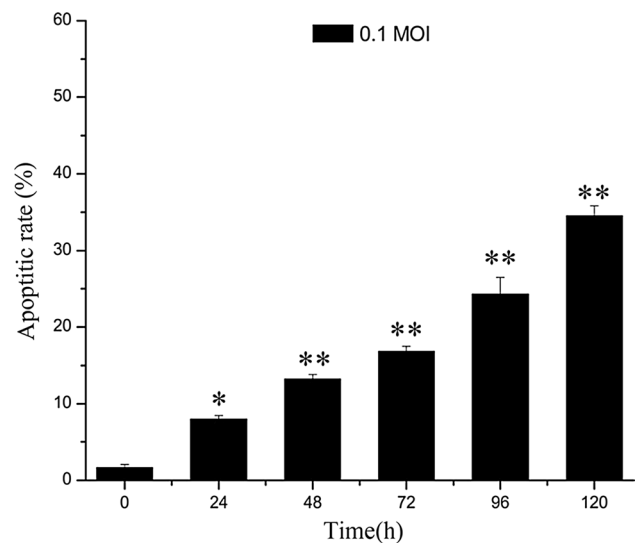
assays showed that the apoptosis rate significantly increased at 24 hpi in PEDV-infected cells when compared with the control group (Fig 1B). CPE appeared at 24 hpi and became obvious at 36 hpi and 48 hpi (Fig 3). These results suggest that PEDV infection induced apoptosis in IECs.

Greater pathogenicity of PEDV proliferation was observed in IEC cells than in Vero cells

All piglets infected with CV777 in group 1 exhibited watery diarrhea and significant emaciation after 24 hours. Piglets in group 2 exhibited no watery diarrhea until 36 hpi, while piglets in the control group still remained healthy at 36 hpi. After two days post-infection, two piglets in group 1 died after exhibiting severe watery diarrhea, while the remaining

Fig. 4 The necropsies result of pigs infected with CV777 harvested from IEC cells (A) and Vero cells (B) and the control group (C)
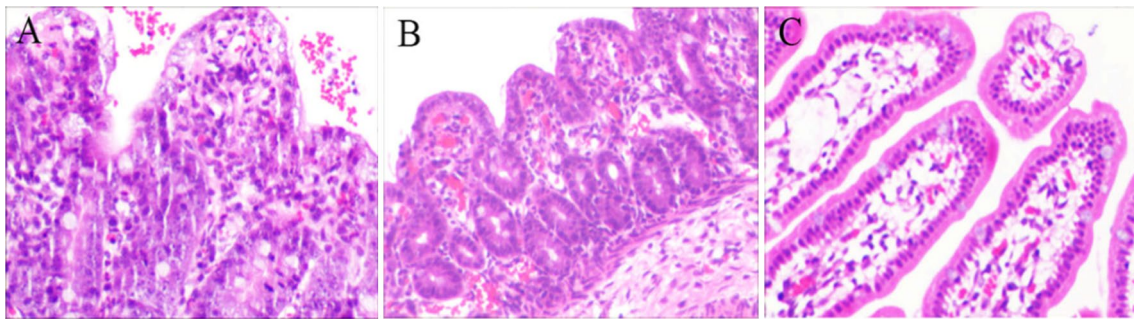

Fig. 5 Hematoxylin and eosin (HE) assay of pigs infected with CV777-IEC (A) and CV777-Vero (B) and control group (C)

infected piglets in the group exhibited typical fluidic diarrhea. The intestinal tract morphologies of nine piglets were analyzed after necropsy (Fig 4). The intestinal tracts of six piglets in group 1 and group 2 were typically distended with yellow watery contents. Clinical symptoms were more obvious and serious in group 1 than in group 2. Meanwhile, piglets in the control group were normal (Fig 4C). The results from HE staining demonstrated significant destruction of cells in infected piglets' intestinal tracts (Fig 5). Pathological symptoms in group 1 were more serious than in group 2 with regard to serious atrophy of mucosal villi, hyperemia of mucosal lamina propria and presence of red blood cells in the lumen. In group 2, the mucosal villi atrophied and the mucosal lamina propria exhibited hyperemia with no red blood cells in the lumen. Meanwhile, control group samples showed healthy villi structures with the orderly arrangement of chorionic epithelial cells. HE staining revealed that villus length and V/C ratio were all markedly reduced, exhibiting significant differences relative to normal tissue features ($P < 0.05$); meanwhile mucosal thickness increased in the experiment group and led to lower level generation of small intestinal epithelial cells and reduction of small intestinal secretory function (Table 4).

According to observations of clinical symptoms and results of necropsies and HE assays of infected piglets, it was concluded that virus virulence of IECs was greater than virulence of virus harvested from Vero cells. Therefore, the

Table 4 The influence of CV777 strains harvested from IEC cells (A) and Vero cells (B) on mucosal layer thickness, villus length and V/C of piglet jejunum. n = 5; *P < 0.05; **P < 0.01

Group	Mucosa thickness (µm)	Villus length (µm)	V/C
A	6.02 ± 0.03**	22.6 ± 0.05**	3.75 ± 0.01**
B	5.77 ± 0.02**	24.2 ± 0.04**	4.19 ± 0.02**
C	5.10 ± 0.05	35.7 ± 0.07	7.0 ± 0.01

results of this study may lay the foundation for further studies to understand PEDV attenuation for potential vaccine development.

Discussion

Since the first known outbreak of PEDV worldwide, researchers have been trying to identify factors permitting viral replication in cultured cells *in vitro*, as PEDV does not readily adapt to achieve infect cultured cells. Prior to 1988, the Swiss researcher M. Hofmann first found that PEDV can successfully replicate in Vero cells (monkey kidney) in culture medium containing trypsin [10]. Subsequently, PEDV was found to also infect Marc-145 (monkey kidney), PK-15 (pig kidney) and Huh-7 (human liver) cells efficiently when cultures were supplemented with trypsin; however,

viral CPE and virus titers differed among various cell types [24]. Apparently, PEDV proliferation is complex *in vitro* and cellular host differences greatly influence the outcome of infection. Consequently, the lack of a suitable experimental host for virus studies has hindered elucidation of virus biological characteristics related to its multiplication and developmental processes that indirectly lead to PED transmission.

In vivo, the PEDV target organ is the small intestine, where virus replication is limited to intestinal villus epithelial cells. Viral damage to these cells causes a breach of mucosal physical barriers and reduces enzyme activities, leading to electrolyte imbalances, nutrient decomposition and absorption anomalies. Such changes ultimately result in increased osmotic pressure of the bowel loops that leads to dehydration and diarrhea. In addition, PEDV infection inhibits the growth of IEC cells, with concomitant increases in cell apoptosis observed. Severe apoptosis can interfere with epithelial mucosal cell function, resulting in a shortening of intestinal villus length that coincides with the appearance of pathological characteristics.

Molecular mechanisms of PED may involve Na^+-K^+-ATPase and Ca^{2+}-Mg^{2+}-ATPase, the most important enzymes among the ATPases. These enzymes are ubiquitous ion pumps that employ active transport of ions to establish ion gradients. In most animal cells, Na^+-K^+-ATPases are cytoplasmic membrane glycoproteins that serve as carrier proteins involved in active transport of Na^+ and K^+ [23]. Ca^{2+}-Mg^{2+}-ATPases, another group of important enzymatic cytoplasmic membrane glycoproteins, also play a role in ion transport. Decreases in Ca^{2+}-Mg^{2+}-ATPase activity reduce ion transport across the membrane barrier, causing Ca^{2+} to accumulate in the cytoplasm that eventually leads to abnormal cell morphology, structure and function. As part of normal gastrointestinal tissue function, Na^+-K^+-ATPase and Ca^{2+}-Mg^{2+}-ATPase are key players that perform active transport-based maintenance of the protective barrier to resist tissue damage. Reduction in activities of ATPases leads to membrane ion pump dysfunction and abnormal Na^+, K^+, Ca^{2+} and Mg^{2+} distribution, eventually resulting in gastric mucosal cell swelling and necrosis [25, 26].

Pig small intestinal mucosal epithelial cells are known natural host cell targets of PEDV infection and thus would be the most useful cells for study of pathogenicity between PEDV and its host. Therefore, IECs derived from these cells were used here to study PEDV pathogenic mechanisms that include direct small intestinal mucosa epithelial cell breakage and death, as well as later effects on intestinal function and activity. Ultimately, the use of *in vitro* IECs has allowed us to demonstrate that ATPase activities appear to be important for small intestine functional changes resulting from PEDV infection. While the enzyme activity of the control group showed little change with time, in the experimental group Na^+-K^+-ATPase activity

was markedly and significantly reduced after infection (P < 0.05). Meanwhile, Ca^{2+}-Mg^{2+}-ATPase activity was also markedly and significantly decreased (P < 0.05). Thus, PEDV infection of pigs resulted in reduction of small intestinal villus epithelial cell ATPases activity, membrane ion pump dysfunction and abnormal Na+, K^+, Ca^{2+} and Mg^{2+} distribution. These ion changes maybe the main factors that lead to gastrointestinal mucosal cell swelling, damage and necrosis.

In pig small intestines, normally approximately 800 to 1200 cells undergo apoptosis daily per intestinal root hair within the small intestinal mucosa. This cell turnover is necessary, as intestinal mucosa must constantly regenerate itself to maintain a mucosal barrier to preserve normal intestinal digestion and absorption abilities. However, PEDV infection reduced proliferation of pig small intestinal villus epithelial cells and concurrently caused increases in observed cell apoptosis. These changes prevented the protective layer of mucosal epithelium from functioning and regenerating itself, resulting in visible shortening of villi. Ultimately, PEDV infection greatly affected normal activities and functions of piglet intestinal mucosal epithelial cells, leading to impaired intestinal digestion and nutrient absorption.

In conclusion, the present study aimed to reveal pathogenic mechanisms contributing to PEDV virulence in target cell IECs. First, we used an immortalized IEC cell line which demonstrated that PEDV can infect IECs, showing extensive viral replication and significant increases in IEC apoptosis. Notably, PEDV isolated after infection of 10-day-old piglets showed a slightly higher level of propagation in IEC cells than in Vero cells overall, with increasingly marked pathogenicity and proliferation observed with greater time post-infection in IEC cells versus Vero cells. Since piglets exhibit watery diarrhea and dehydration post-PEDV infection, we studied Na^+-K^+-ATPase and Ca^{2+}-Mg^{2+}-ATPase activities in IECs and demonstrated significant alterations of Na (+), K (+) and Ca (2+) content that mirrored observed decreases in enzyme activities. The results of this study should therefore stimulate future research to prevent, detect and treat PEDV infection in pigs and develop attenuated PEDV vaccines.

Compliance with ethical standards

Conflicts of interest The authors declare that there are no conflicts of interest in this paper.

References

1. Wood EN (1977) Apparently new syndrome of porcine epidemic diarrhea. Vet Rec 100:243–244

2. Song D, Park B (2012) Porcine epidemic diarrhea virus: a comprehensive review of molecular epidemiology, diagnosis, and vaccines. Virus Genes 44:167–175. https://doi.org/10.1007/s11262-012-0713-1

3. Jung K, Saif LJ (2015) Porcine epidemic diarrhea virus infection: etiology, epidemiology, pathogenesis and immunoprophylaxis. Vet J 204:134–143. https://doi.org/10.1016/j.tvjl.2015.02.017

4. Kim YK, Lim SI, Cho IS, Cheong KM, Lee EJ, Lee SO, Kim JB, Kim JH, Jeong DS, An BH, An DJ (2015) A novel diagnostic approach to detecting porcine epidemic diarrhea virus: the lateral immunochromatography assay. J Virol Methods 225:4–8. https://doi.org/10.1016/j.jviromet.2015.08.024

5. Wang XY, Ji CJ, Zhang X, Xu DP, Zhang DL (2017) Infection, genetic and virulence characteristics of porcine epidemic diarrhea virus in northwest China. Infect Genet Evol 62:34–39. https://doi.org/10.1016/j.meegid.2018.04.001

6. Li Y, Zheng F, Fan B, Muhammad HM, Zou Y, Jiang P (2015) Development of an indirect ELISA based on a truncated S protein of the porcine epidemic diarrhea virus. Can J Microbiol 61:811–817. https://doi.org/10.1139/cjm-2015-0213

7. Zhang X, Hao J, Zhen J, Yin L, Li Q, Xue C, Cao Y (2015) Rapid quantitation of porcine epidemic diarrhea virus (PEDV) by Virus Counter. J Virol Methods 223:1–4. https://doi.org/10.1016/j.jviromet.2015.07.003

8. Huang YW, Dickerman AW, Piñeyro P, Li L, Fang L, Kiehne R, Opriessnig T, Meng XJ (2013) Origin, evolution, and genotyping of emergent porcine epidemic diarrhea virus strains in the United States. MBio 4:e00737–e00813. https://doi.org/10.1128/mBio.00737-13

9. Lee S, Lee C (2014) Outbreak-related porcine epidemic diarrhea virus strains similar to US strains, South Korea, 2013. Emerg Infect Dis 20:1223–1226. https://doi.org/10.3201/eid2007.140294

10. Hofmann M, Wyler R (1988) Propagation of the virus of porcine epidemic diarrhea in cell culture. J Clin Microbiol 26:2235–2239

11. Shi W, Jia S, Zhao H, Yin J, Wang X, Yu M, Ma S, Wu Y, Chen Y, Fan W, Xu Y, Li Y (2017) Novel approach for isolation and identification of porcine epidemic diarrhea virus (PEDV) strain NJ using porcine intestinal epithelial cells. Viruses E9:19

12. Wang J, Hu G, Lin Z, He L, Xu L, Zhang Y (2014) Characteristic and functional analysis of a newly established porcine small intestinal epithelial cell line. PLoS One 9:e110916. https://doi.org/10.1371/journal.pone.0110916

13. Pavlov KV, Sokolov VS (2000) Electrogenic ion transport by Na^+, K^+-ATPases. Membr Cell Bio 13:745–788

14. Kaunitz JD (2006) Membrane transport proteins: not just for transport anymore. Am J Physiol Renal Physiol 290:F995–F996

15. Norouzi-Javidan A, Javanbakht J, Barati F, Fakhraei N, Mohammadi F, Dehpour AR (2015) Serotonin 5-HT7 receptor agonist, LP-211, exacerbates $Na(^+)$, $K(^+)$-ATPase/$Mg(^{2+})$-ATPase imbalances in spinal cord-injured male rats. Diagn Pathol 10:157. https://doi.org/10.1186/s13000-015-0397-7

16. Robinson JD, Flashner MS (1979) The $(Na^+ + K^+)$-activated ATPase. Enzymatic and transport properties. Biochim Biophys Acta 549:145–176

17. Chauhan NB, Lee JM, Siegel GJ (1997) Na, K-ATPase mRNA levels and plaque load in Alzheimer's disease. J Mol Neurosci 9:151–166

18. Rose AM, Valdes R Jr (1994) Understanding the sodium pump and its relevance to disease. Clin Chem 40:1674–1685

19. Shah S, Kongre V, Kumar V, Bharadwaj R (2016) A study of parasitic and bacterial pathogens associated with diarrhea in HIV-positive patients. Cureus 8:e807

20. Zhao J, Shi BJ, Huang XG, Peng MY, Zhang XM, He DN, Pang R, Zhou B, Chen PY (2013) A multiplex RT-PR assay for rapid and differential diagnosis of four porcine diarrhea associated viruses in field samples from pig farms in East China from 2010 to 2012. J Virol Methods 194:107–112. https://doi.org/10.1016/j.jviromet.2013.08.008

21. Reed LJ, Muench H (1938) A simple method of estimating fifty per cent endpoints. Am J Hyg 27:493–497

22. Ding L, Xu X, Huang Y, Li Z, Zhang K, Chen G, Yu G, Wang Z, Li W, Tong D (2012) Transmissible gastroenteritis virus infection induces apoptosis through FasL-and mitochondria-mediated pathways. Vet Microbiol 158:12–22. https://doi.org/10.1016/j.vetmic.2012.01.017

23. Manoharan P, Gayam S, Arthur S, Palaniappan B, Singh S, Dick GM, Sundaram U (2015) Chronic and selective inhibition of basolateral membrane Na-K-ATPase uniquely regulates brush border membrane Na absorption in intestinal epithelial cells. Am J Physiol Cell Physiol 308:C650–C656. https://doi.org/10.1152/ajpcell.00355.2014

24. Wang J, Deng F, Ye G, Dong W, Zheng A, He Q, Peng G (2016) Comparison of lentiviruses pseudotyped with S proteins from coronaviruses and cell tropisms of porcinecoronaviruses. Virol Sin 31:49–56. https://doi.org/10.1007/s12250-015-3690-4

25. Xiong X, Yang H, Hu X, Wang X, Li B, Long L, Li T, Wang J, Hou Y, Wu G, Yin Y (2016) Differential proteome analysis along jejunal crypt-villus axis in piglets. Front Biosci (Landmark Ed) 21:343–363

26. Ziegelhoffer A, Kjeldsen K, Bundgaard H, Breier A, Vrbjar N, Dzurba A (2000) Na, K-ATPase in the myocardium: molecular principles, functional and clinical aspects. Gen Physiol Biophys 19:9–47